Application of Maximum Likelihood Method for the Analysis of Spin Density Matrix Elements of Vector Meson Production at HERMES

A.Borissov

Department of Physics and Astronomy, University of Glasgow, Glasgow, G128QQ, United Kingdom
E-mail: *borissov@mail.desy.de*

April 28, 2006

Abstract. Spin Density Matrix Elements (SDMEs) have been determined from exclusive diffractive ρ^0 production in the HERMES experiment at 27.5 GeV beam energy. Beam polarization dependent and independent SDMEs have been extracted from the data on hydrogen and deuterium targets accumulated in the years 1996 - 2000 in the HERMES kinematic region $1 < Q^2 < 5$ GeV^2, $3.0 < W < 6.3$ GeV using maximum likelihood method. A small but statistically significant violation of s-Channel Helicity Conservation (SCHC) is observed.

Exclusive leptoproduction of a ρ^0 vector meson in the intermediate energy region, as for the HERMES experiment, is of particular interest. Two mechanisms are involved in the interaction of the virtual photon with the nucleon. While the Pomeron or two-gluon exchange dominates at higher energies, the quark-exchange mechanism becomes important only at intermediate energies. As can be seen from Fig.1, studying the s-channel of the process $\gamma^* p \to \rho^0 p$ provides information on the nature of vector meson formation.

The measurement of the scattered lepton and of the decay products of the vector meson allows the reconstruction of the full reaction kinematics and the determination of the vector meson decay distributions. From this information the 15 'unpolarized' Spin Density Matrix Elements (SDMEs) can be determined. The full set of 23 SDMEs, including the 8 'polarized' ones, can be extracted only if the information on the longitudinal polarization of the HERA lepton beam at HERMES is exploited.

SDMEs are usually described in the center-of-mass system of virtual photon and proton by helicity amplitudes $T_{\lambda_V \lambda'_N, \lambda_\gamma \lambda_N}$ where λ_V (λ_γ) is the helicity of the vector meson (virtual photon) and λ_N, λ'_N denote the helicities of the incident and the outgoing nucleon, respectively.

The spin density matrix elements $\rho^\alpha_{\lambda_V \lambda'_V}$ of a vector meson are given by [1]:

$$\rho^\alpha_{\lambda_V \lambda_{V'}} = \frac{1}{2N_\alpha} \sum_{\lambda_\gamma \lambda_{\gamma'}} T_{\lambda_V \lambda_\gamma} \Sigma^\alpha_{\lambda_\gamma \lambda'_\gamma} T^*_{\lambda'_V \lambda'_\gamma}, \qquad (1)$$

for $\alpha = 0, 1, \ldots, 8$. Here N_α are normalization factors (N_L and N_T for longitudinal and transverse virtual photons, respectively) and $\Sigma^\alpha_{\lambda_\gamma \lambda'_\gamma}$ are nine hermitian matrices defined in Ref. [1]. The helicity amplitudes have been defined

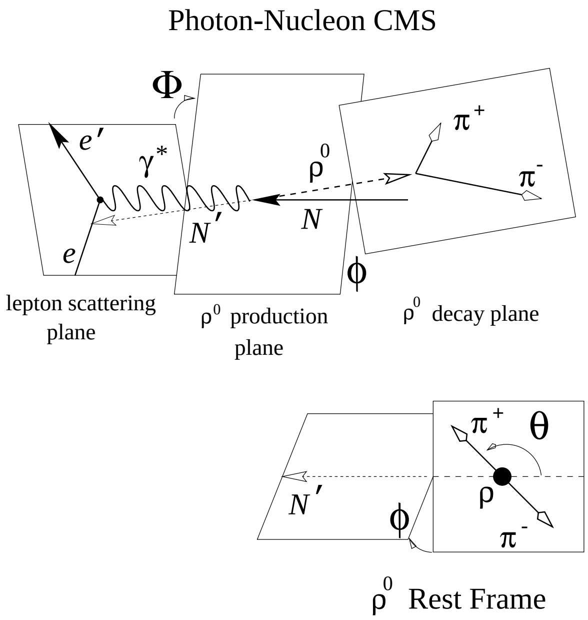

Fig. 1. The definition of angles used in ρ^0 SDME analysis: Φ is the angle between scattering plane and ρ^0 production plane, Θ and ϕ are polar and azimuthal angle of the decay π^+ in the vector meson rest frame with z-axis aligned opposite to outgoing nucleon momentum in the center of mass of γ^* p system.

in Ref. [2]:

$$T_{\lambda_V \lambda'_N, \lambda_\gamma \lambda_N} = \langle \lambda_V \lambda'_N | (J \cdot e^{(\lambda_\gamma)}) | \lambda_N \rangle, \qquad (2)$$

where J is the electromagnetic current vector and $e^{(\lambda_\gamma)}$ denotes the virtual photon polarization vector ($\lambda_\gamma = 0$

for longitudinal and $\lambda_\gamma = \pm1$ for transverse polarization). The initial (λ_N) and final nucleon helicities (λ'_N) are summed over.

SDMEs describe vector meson formation from both transverse and longitudinal virtual photons. By convention, $\alpha = 0, 1, 2, 3$ in Eq. (1) represent transverse-photon polarization states (unpolarized, two directions of linear polarization, circular polarization). For these cases, $N_\alpha = N_T$. Pure longitudinal photons are denoted by $\alpha = 4$ with $N_\alpha = N_L$. The cases $\alpha = 5, 6, 7, 8$ are attributed to the interference of longitudinal and transverse photons, with $N_\alpha = \sqrt{N_L N_T}$.

If the produced vector meson has the same helicity as the virtual photon and the proton helicity is unchanged (s-channel helicity conservation, SCHC), certain SDMEs vanish:

$$T_{\lambda_V \lambda'_N, \lambda_\gamma \lambda_N} = T_{\lambda_V \lambda'_N, \lambda_\gamma \lambda_N} \delta_{\lambda_V \lambda_\gamma} \delta_{\lambda'_N \lambda_N}, \tag{3}$$

with δ_{jk} being the Kronecker symbol. In this case all helicity-flip amplitudes vanish,

$$T_{01} = T_{10} = T_{-10} = T_{0-1} = T_{-11} = T_{1-1} = 0, \tag{4}$$

so that only three independent amplitudes remain: T_{00}, T_{11}, T_{-1-1}. In consequence all matrix elements vanish, except r^{04}_{00}, Re$\{r^1_{1-1}\}$, Im$\{(r^2_{1-1}\}$, Re$\{r^5_{10}\}$, Im$\{r^6_{10}\}$, Im$\{r^7_{10}\}$ and Re$\{r^8_{10}\}$.

The HERMES experiment at DESY uses a 27.5 GeV longitudinally polarized positron beam impinging on hydrogen or deuterium gas targets internal to the HERA storage ring. Part of the data sets was collected with longitudinally polarized targets. Since the target polarization is not exploited in the present analysis, an average over both target polarization states is taken. The lepton beam is transversely self-polarized by the emission of synchrotron radiation Ref. [3]. The longitudinal polarization at the interaction point is obtained by spin rotators located upstream and downstream of the HERMES experiment. The beam polarization was continuously measured by two Compton polarimeters [4,5]. The average beam polarization for the proton (deuteron) data set was 0.53 (0.53) for both positive and negative beam helicities after requiring $0.3 < P_{beam} < 0.8$. The fractional systematic uncertainty of the beam polarization is 3.4% (2.0%) [4,5].

The HERMES spectrometer is presented in Fig.2 and described in detail in Ref. [6]. It is a forward spectrometer in which both scattered positron and produced hadrons are detected within an angular acceptance ± 170 mrad horizontally, and ± (40 - 140) mrad vertically. The scattered-positron trigger was formed from a coincidence between a pair of scintillator hodoscope planes and a lead-glass calorimeter. The trigger required an energy of more than 3.5 GeV deposited in the calorimeter. The tracking system has a momentum resolution of about 1.5 % and an angular resolution of about 1 mrad. Positron identification was accomplished using a lead-glass calorimeter, a preshower detector consisting of a scintillator hodoscope preceded by a lead sheet, and a transition-radiation detector. Until 1998 the particle identification system included a gas threshold Čerenkov counter, which was replaced by a dual-radiator ring-imaging Čerenkov detector (RICH) [7] for data from 1999. Combining the responses of these detectors in a likelihood method leads to an average electron (positron) identification efficiency of 98% with a hadron contamination of less than 1%.

The exclusive rho^0 events were selected in the same procedure as described in Ref.[8,9]. The SDMEs are obtained directly from the measured angular distributions by minimizing the difference between the 3-dimensional $(\cos\Theta, \phi, \Phi)$ decay angle matrix of the data and that of a sample of fully reconstructed Monte Carlo events, using the maximum likelihood method. The variables $\cos\Theta$, ϕ, Φ are binned in $8 \times 8 \times 8$ bins. The Monte Carlo events are generated starting from isotropic angular distributions in 4π and passed through the same reconstruction chain as the experimental data. The fit is done in an iterative procedure, using Eq. (5) for Monte Carlo event weighting, whereby the 23 matrix elements are treated as free parameters. The best fit parameters are determined using a binned maximum log-likelihood method. The number of events in each bin is assumed to obey a Poisson distribution. The likelihood function was defined in Ref. [10]. The minimization itself and the error calculation were performed using the MINUIT package [11]. In the fitting procedure the samples with negative and positive beam helicity were fitted simultaneously, using the common set of 23 parameters. The isotropic input distributions are shown as modified by spectrometer acceptance and reconstruction procedure. The fitted angular dependences reproduce the data very well, as can be seen from the figure. As a systematic check, both helicity samples are fitted separately giving fully consistent results.

In Fig. 3 are shown the spin density matrix elements as obtained from separate likelihood fits to the proton and deuteron data samples for the kinematic region: $1.0 < Q^2 < 5.0$ GeV^2, $3.0 < W < 6.3$ GeV and $0.03 < x < 0.25$. The inner error bars correspond to the statistical uncertainties as given by MINUIT. The outer error bars correspond to total uncertainties calculated as a quadratic superposition of statistical and systematic uncertainties. The statistical uncertainties are larger for the eight polarized SDMEs (shown in the bottom of the figure) due to the fact that the lepton beam polarization amounts to about 53%.

The deviations from the SCHC expectations are shown in Fig. 3 by enlarged symbols. The results indicate a significant violation of the assumption of s-channel helicity conservation. The element r^5_{00} is found to deviate from zero by about five standard deviations for both hydrogen and deuterium targets. This matrix element is proportional to the interference between the helicity-conserving longitudinal amplitude T_{00} and the single-flip amplitude T_{01}, see Fig. 3. The latter amplitude corresponds to the production of longitudinally polarized ρ^0 mesons from transverse photons. About four standard deviations from zero is observed for the elements Re$\{r^{04}_{10}\}$ and Re$\{r^1_{10}\}$, which also

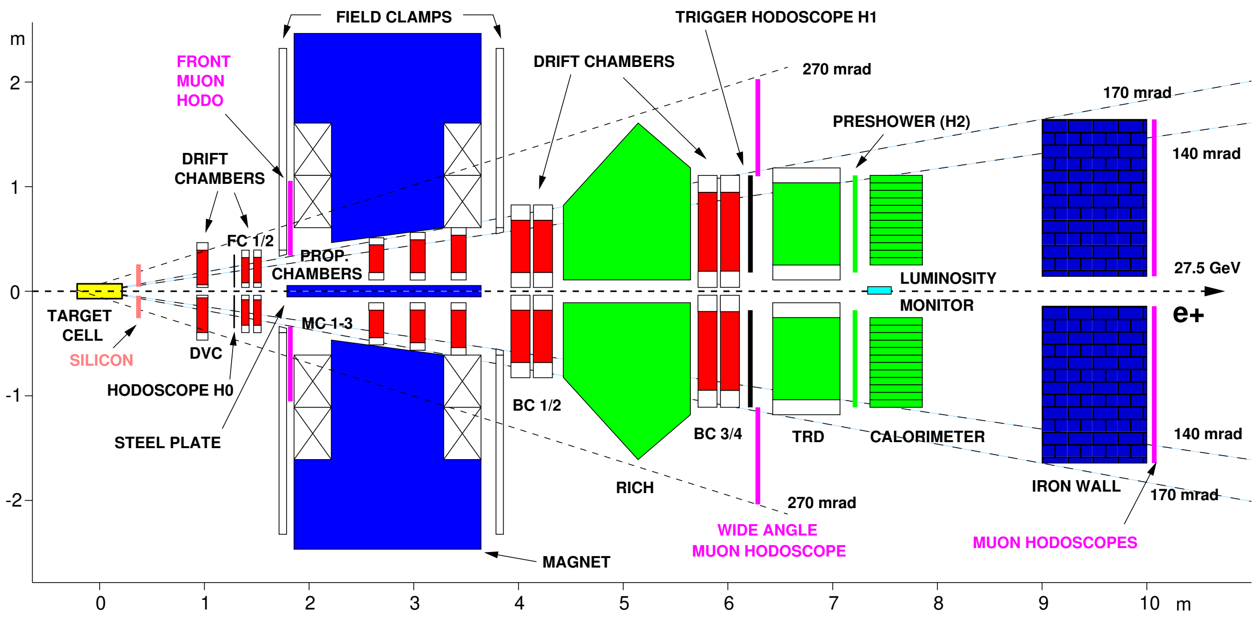

Fig. 2. Schematic side view of HERMES spectrometer.

$$\mathrm{W}(\cos\Theta,\phi,\Phi) = W^{unpol} + W^{long.pol},$$

$$\mathrm{W}^{unpol}(\cos\Theta,\phi,\Phi) = \tfrac{3}{8\pi^2}\Bigg[\tfrac{1}{2}(1-r^{04}_{00}) + \tfrac{1}{2}(3r^{04}_{00}-1)\cos^2\Theta - \sqrt{2}\mathrm{Re}\{\mathrm{r}^{04}_{10}\}\sin 2\Theta\cos\phi - \mathrm{r}^{04}_{1-1}\sin^2\Theta\cos 2\phi$$

$$-\ \epsilon\cos 2\Phi\Big(r^1_{11}\sin^2\Theta + r^1_{00}\cos^2\Theta - \sqrt{2}\mathrm{Re}\{\mathrm{r}^1_{10}\}\sin 2\Theta\cos\phi - \mathrm{r}^1_{1-1}\sin^2\Theta\cos 2\phi\Big)$$

$$-\ \epsilon\sin 2\Phi\Big(\sqrt{2}\mathrm{Im}\{\mathrm{r}^2_{10}\}\sin 2\Theta\sin\phi + \mathrm{Im}\{\mathrm{r}^2_{1-1}\}\sin^2\Theta\sin 2\phi\Big)$$

$$+\ \sqrt{2\epsilon(1+\epsilon)}\cos\Phi\Big(r^5_{11}\sin^2\Theta + r^5_{00}\cos^2\Theta - \sqrt{2}\mathrm{Re}\{\mathrm{r}^5_{10}\}\sin 2\Theta\cos\phi - \mathrm{r}^5_{1-1}\sin^2\Theta\cos 2\phi\Big)$$

$$+\ \sqrt{2\epsilon(1+\epsilon)}\sin\Phi\Big(\sqrt{2}\mathrm{Im}\{\mathrm{r}^6_{10}\}\sin 2\Theta\sin\phi + \mathrm{Im}\{\mathrm{r}^6_{1-1}\}\sin^2\Theta\sin 2\phi\Big)\Bigg],$$

$$\mathrm{W}^{long.pol.}(\cos\Theta,\phi,\Phi) = \tfrac{3}{8\pi^2}P_{beam}\Bigg[\sqrt{1-\epsilon^2}\Big(\sqrt{2}\mathrm{Im}\{\mathrm{r}^3_{10}\}\sin 2\Theta\sin\phi + \mathrm{Im}\{\mathrm{r}^3_{1-1}\}\sin^2\Theta\sin 2\phi\Big)$$

$$+\ \sqrt{2\epsilon(1-\epsilon)}\cos\Phi\Big(\sqrt{2}\mathrm{Im}\{\mathrm{r}^7_{10}\}\sin 2\Theta\sin\phi + \mathrm{Im}\{\mathrm{r}^7_{1-1}\}\sin^2\Theta\sin 2\phi\Big)$$

$$+\ \sqrt{2\epsilon(1-\epsilon)}\sin\Phi\Big(r^8_{11}\sin^2\Theta + r^8_{00}\cos^2\Theta - \sqrt{2}\mathrm{Re}\{\mathrm{r}^8_{10}\}\sin 2\Theta\cos\phi - \mathrm{r}^8_{1-1}\sin^2\Theta\cos 2\phi\Big)\Bigg] \quad (5)$$

are correlated with the T_{01} amplitude [12]. Seven other elements differ from zero by about two standard deviations. Note that in the fit of Monte Carlo events simulated under the SCHC assumption all the expected elements are found to be consistent with zero.

The above results confirm the non-zero value of r^5_{00} found in Refs. [12–15]. Owing to the improved accuracy of this data, for the first time other non-zero SCHC-violating SDMEs are identified, see enlarged symbols in Fig. 3. The following unpolarized SDMEs have significantly non-zero values: $\mathrm{Re}\{r^{04}_{10}\}$, $\mathrm{Re}\{r^1_{10}\}$, $\mathrm{Im}\{r^2_{10}\}$. The polarized elements $\mathrm{Im}\{r^3_{10}\}$, r^8_{00}, $\mathrm{Im}\{r^7_{1-1}\}$ are found to be non zero. These results emphasize that in the intermediate energy domain SCHC is violated and spin-flip amplitudes contribute to exclusive ρ^0 production.

References

1. K. Schilling and G.Wolf, Nucl. Phys. **B61** (1973) 381
2. M.Jacob and G.C.Wick, Ann.Phys. **7** (1959) 404
3. A.Sokolov, I.Ternov, Sov. Phys. Doklagy **8** (1964) 1203
4. D.P.Barber et al., Nucl. Instr. and Meth. **A 329** (1993) 79

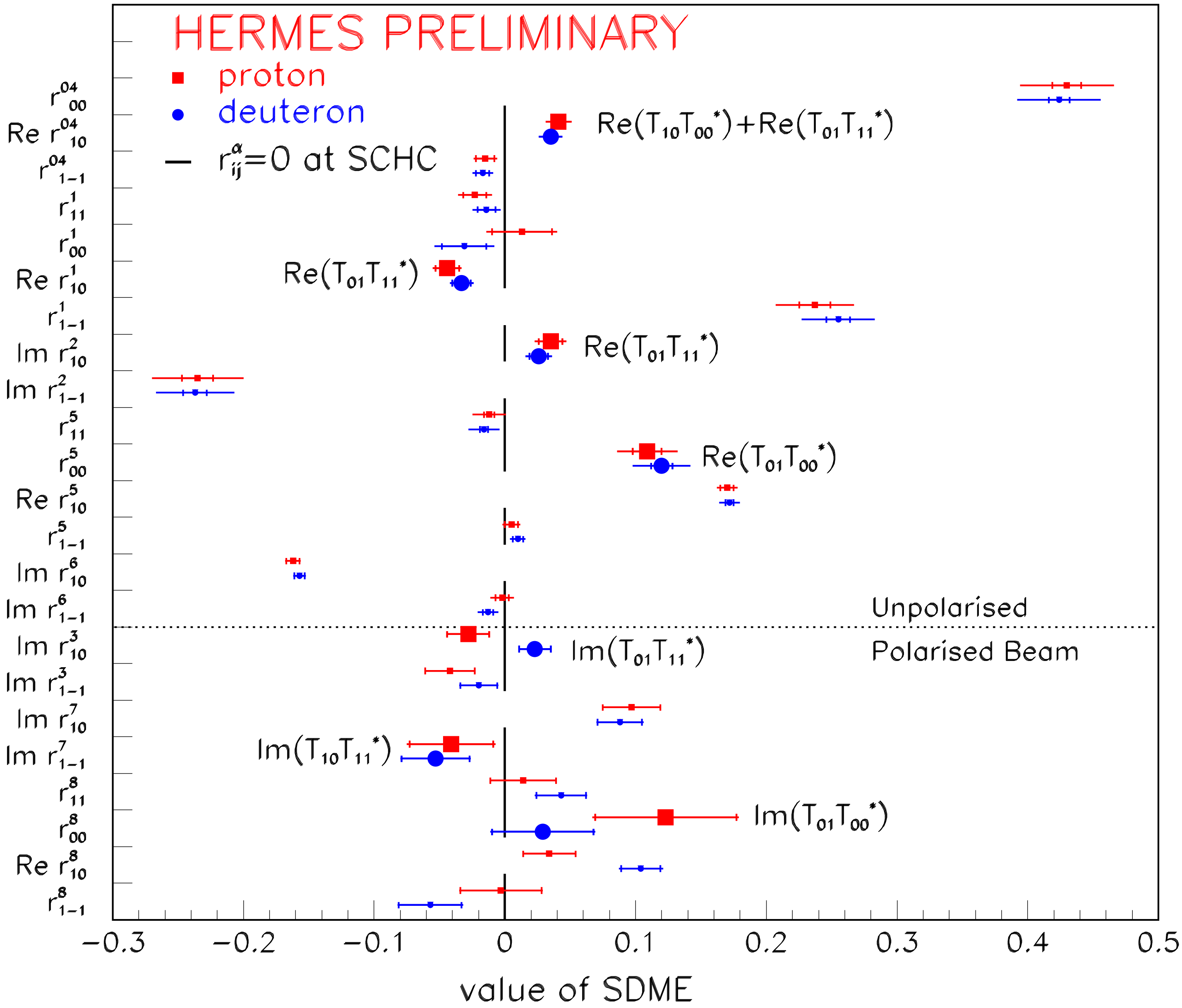

Fig. 3. The 23 spin density matrix elements extracted from ρ^0 data, red squares for proton and blue circles for deuteron. The inner error bars represent the statistical uncertainty, while the outer ones indicate the statistical and systematic uncertainties added in quadrature. SDMEs measured with unpolarized (polarized) beam are displayed above (below) the dotted line. The enlarged symbols indicate those SDMEs which are restricted by SCHC to be zero.

5. M.Beckmann et al., Nucl. Instr. and Meth. **A 479** (2002) 334
6. HERMES Collab. K.Ackerstaff et al, NIM A **417** (1998) 230
7. N.Akopov et al., Nucl. Instr. and Meth. **A 479** (2002) 511
8. A. Airapetian et al, Eur. Phys. Jour. C **17** (2000) 3898
9. K. Ackerstaff et al., Eur. Phys. J. C **18** (2000) 303
10. G.Zech, DESY-Report 95-115
11. CERN-CN Division, CERN Program Library Long Writeup **D506** (1992)
12. J. Breitweg et.al., ZEUS Coll., Eur. Phys. J. **C12** (2000) 393
13. C. Adloff et al., H1 Coll., Eur. Phys. J. **C13** (2000) 371
14. M.Tytgat, Ph.D. thesis, Gent University (2001), DESY-THESIS-2001-014
15. C. Shearer, Ph.D. thesis, University of Glasgow (2005)